General Circulation Model Sensitivity to 1982–83 Equatorial Pacific Sea Surface Temperature Anomalies

M. J. FENNESSY, L. MARX AND J. SHUKLA

Center for Ocean–Land–Atmosphere Interactions, Department of Meteorology, The University of Maryland, College Park, MD 20742

(Manuscript received 19 July 1984, in final form 5 February 1985)

ABSTRACT

Three control and anomaly simulation pairs run with the Goddard Laboratory for Atmospheric Sciences (GLAS) climate model have been analyzed in order to investigate the atmospheric response to the 1982–83 tropical sea surface temperature anomalies. The observed 1982–83 SST anomalies obtained from the Climate Analysis Center were applied to two separate 75-day control simulations, starting on 16 December 1982 and 16 December 1979, respectively, and a third 60-day control simulation starting on 1 January 1975.

In each experiment the equatorial Pacific precipitation increased significantly in a wide band stretching from just east of the dateline to the South American coast, in agreement with observed outgoing longwave radiation (OLR) anomalies. West of this region the precipitation was reduced in the anomaly simulations. As in previous GCM experiments, the major contributor to the tropical precipitation changes was the low-level moisture convergence. The largest evaporation differences were around 4 mm day^{-1} and occurred over the regions of highest SST in the anomaly simulations. The tropical sea-level pressure field showed a marked Southern Oscillation pattern, with a magnitude of roughly 2 millibars and a node at the dateline. There was a strong ($\sim$10 m s^{-1}) increase in the equatorial eastern Pacific 850 mb westerlies as well as a large (approximately $-$20 m s^{-1}) easterly wind anomaly at 200 mb. The latter anomaly was flanked by strong ($\sim$20 m s^{-1}) westerly anomalies at roughly 30°S and 30°N.

In agreement with earlier simulations with composite SST anomalies, the tropical precipitation anomalies for 1982–83 were also closely related to the extent of very warm ($\geq$29°C) sea surface waters.

Each experiment had anomalous anticyclonic circulations aloft straddling the equator in the eastern Pacific, although they were weaker and more eastward than those observed. The extratropical response varied between the three experiments, as well as between months of a given experiment. Over North America the ensemble average anomaly minus control 300 mb geopotential height difference field resembled the observed February or March anomaly field more than the typical PNA-like pattern. Other extratropical responses were difficult to interpret, although they were clearly equivalent barotropic in structure and showed a much stronger dependence on initial conditions than was noted for the tropics.

1. Introduction

As documented by the Climate Analysis Center (CAC), the warm El Niño sea surface temperature (SST) event of 1982–83 is outstanding in comparison to earlier events. The mature phase SST anomalies were of record magnitude and extent, with greater than 3°C anomalies extending from the South American coast to 150°W in January (Fig. 1a). The January outgoing longwave radiation (OLR) anomaly field depicted a large region of increased convective activity from 160°E to 100°W along the equator (Fig. 2). The Southern Oscillation Index [SOI, Tahiti minus Darwin sea level pressure (SLP)] reached a record low, and a record negative Northern Hemisphere 700 mb height anomaly was observed in the northeast Pacific. For a complete documentation of the evolution of these and other observed climatic anomalies see the CAC special Climate Diagnostics bulletins (1982–83) and Quiroz (1983).

Several general circulation model (GCM) studies (Rowntree, 1972; Julian and Chervin, 1978; Keshavamurty, 1982; Blackmon *et al.*, 1983; Shukla and Wallace, 1983) simulated many of the basic features of the observed atmospheric response to SST anomalies representative of the mature stage of previous El Niño events. The tropical features included an eastward shift of the region of maximum convective activity, increased low-level equatorial Pacific westerlies, and anomalous anticyclonic couplets straddling the equator aloft. The most pronounced extratropical anomaly observed was also simulated, that being the Pacific–North American (PNA) pattern (Wallace and Gutzler, 1981) in the upper-level geopotential height field over the northeast Pacific and North America. Although the general features of the "composite El Niño event" were correctly simulated in most of these experiments, significant variations between experiments utilizing different initial conditions were noted (Shukla and Wallace, 1983).

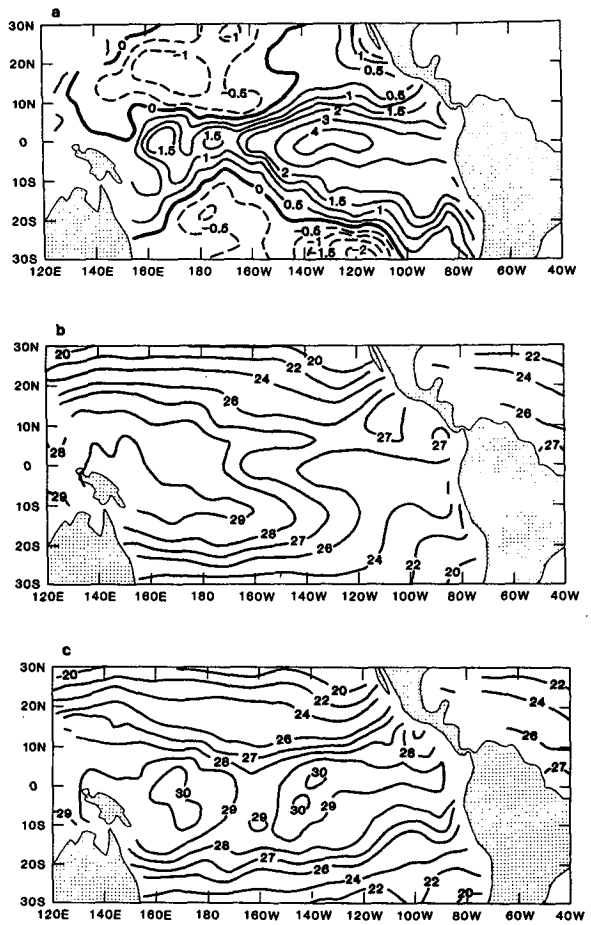

FIG. 1. January 1983 sea surface temperature fields for (a) anomaly-minus-control differences, (b) control simulation and (c) anomaly simulation. (anomaly obtained from CAC). Units are °C. Dashed contours are negative.

The current study examines the response of the GLAS climate model to the much larger 1982–83 SST anomalies as obtained from CAC.

2. Model and integrations

The model is an improved version of the GLAS climate model used by Shukla and Wallace (1983) and documented by Shukla *et al.* (1981). A thorough description of the model and its climatology is given by Randall (1982). It is global in extent with a 4° latitude × 5° longitude grid in the horizontal. Its nine sigma layers of equal thickness are centered at approximately 65, 175· · ·, 945 mb. A Matsuno scheme is used for time integration, and a Shapiro filter is applied at each model half-hour to the pressure, potential temperature, and wind fields. To maintain stability near the poles, Fourier filtering of the zonal wind flux and pressure gradient terms is performed at each time step (7½ minutes). This is preferable to the split-grid used earlier which generated spurious flow components. The planetary boundary layer (PBL) parameterization was also changed to that of Deardorff (1972) as modified by Randall (1976). The model generates supersaturation clouds at all 9 levels and cumulus clouds (Arakawa, 1969) at the lowest 6 levels. In the current version only the supersaturation clouds are allowed to interact with radiation. Shortwave radiation and other physical processes are determined at each model simulated half-hour. Longwave radiation is calculated at 5-hour intervals and applied each half-hour. Dry convective adjustment is performed at each time step. Also differing from the earlier version is the ground hydrology, which carries two temperatures, the ground temperature and saturated ground temperature (Mintz and Serafini, 1981), and the prognostic temperature variable is θ instead of T.

The climatological boundary condition datasets for control integrations are unchanged from those used by Shukla and Wallace (1983) and Shukla *et al.* (1981). Surface albedos are prescribed for land, ocean and desert grid points. Climatological monthly mean sea surface temperatures are interpolated to their daily values.

Important improvements in the current GLAS climate model simulations are the removal of the climate drift towards unrealistically high temperatures in the tropics, noted by Shukla and Wallace (1983), as well as a more realistic sea level pressure pattern. Further details of the models' climatology can be found in Randall (1982).

Three separate experiments (control and anomaly simulation pairs) designed to simulate the mature phase of the 1982–83 event were performed with the following initial conditions: 1) observed initial conditions on 16 December 1982 for 75 days; 2) initial conditions on 16 December 1979 taken from a 2-year model control run after one year of simulation for 75 days; 3) observed initial conditions on 1 January 1975 for 60 days. The January control and anomaly SST fields used in each experiment are shown in Figs. 1b and 1c, respectively. Notable is the greatly extended region of very warm (≥29°C) SST water in the anomaly simulation. The January SST anomaly field is representative of the other months of the experiments, all of which had a much larger

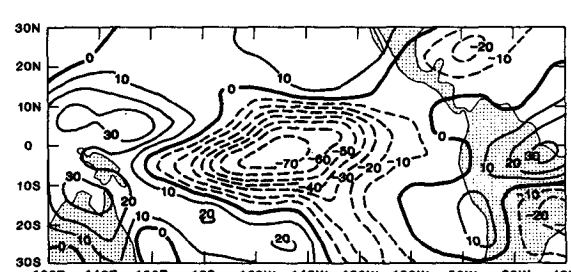

FIG. 2. January 1983 observed outgoing longwave radiation anomaly. Units are W m^{-2}. Obtained from Lau and Chan (from NOAA Polar Orbiters). Dashed contours are negative.

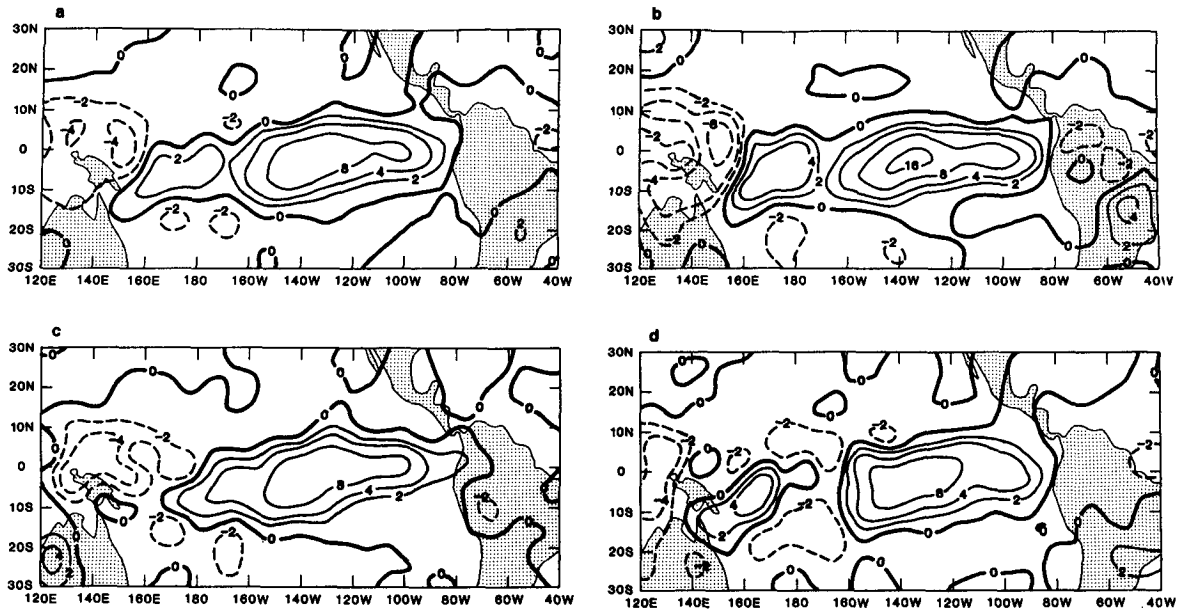

FIG. 3. 11–60 day average anomaly-minus-control precipitation difference for (a) ensemble average, (b) 1982 IC, (c) 1979 IC and (d) 1975 IC. Units are mm day^{-1}.

region of very warm SST in the anomaly simulation than in the previously noted GCM studies.

3. Results

Most of the differences (anomaly minus control) were quite similar in the three experiments, thus we will concentrate on averages of all three and refer to this as the ensemble average. We will note any

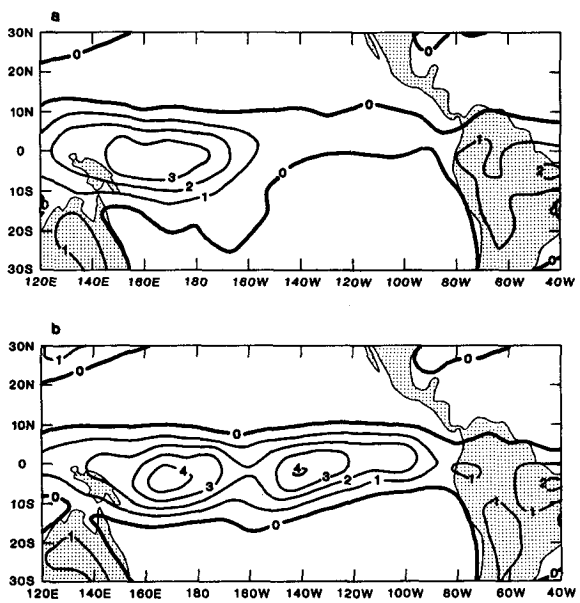

FIG. 4. 11–60 day ensemble average modeled total atmospheric diabatic heating field for (a) control and (b) anomaly. Units are °C day^{-1}.

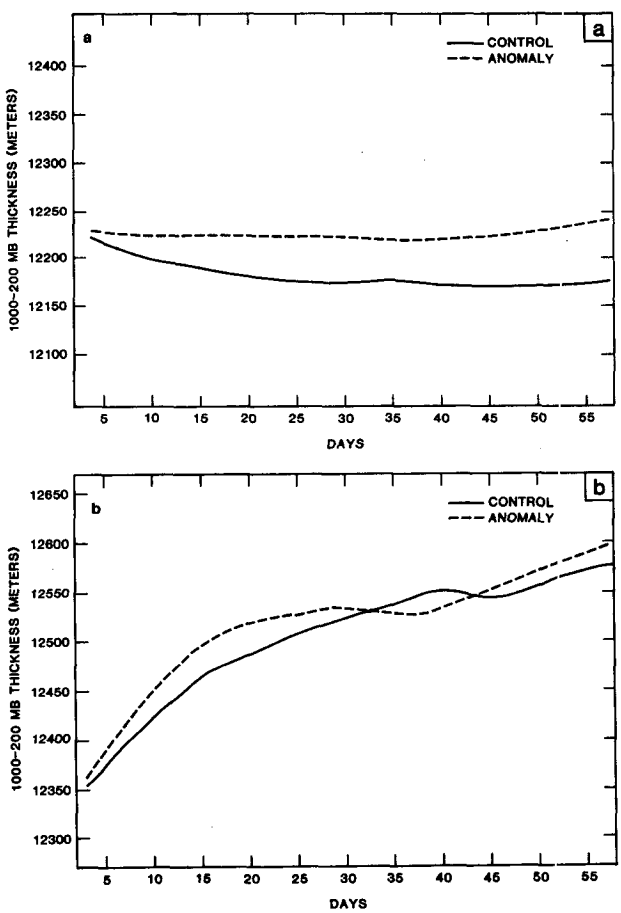

FIG. 5. Zonally averaged 30°N–30°S 200–1000 mb thickness 5-day running mean time series for (a) ensemble average and (b) Shukla and Wallace (1983). Units are geopotential meters.

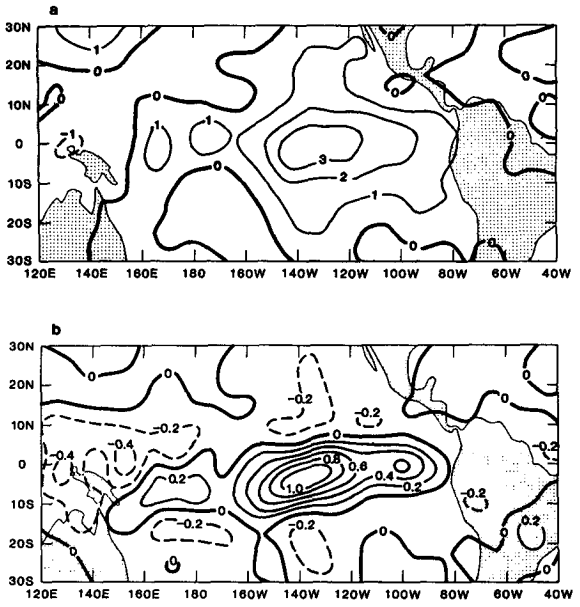

FIG. 6. 11–60 day ensemble average anomaly-minus-control (a) evaporation difference. Units are mm day^{-1}. (b) Vertically integrated moisture convergence difference. Units are g Kg^{-1} day^{-1}. Dashed contours are negative.

appreciable individual departures from the ensemble averages when they occur.

a. Precipitation and heating

The ensemble average 11–60 day precipitation difference field (hereafter differences referenced are anomaly minus control) shown in Fig. 3a exhibits a wide region of enhanced precipitation from 160°E to 80°W in the anomaly simulation, as well as a region of decreased precipitation to the west. These differences, as well as the positive differences over SW Brazil and the Gulf of Mexico agree well with the CAC January 1983 OLR anomalies (Fig. 2). The exceptions are the eastward extension of the simulated anomaly and the failure to capture the observed anomalous precipitation to the southeast, associated with a shift in the South Pacific Convergence Zone. However, the overall similarity between the simulated precipitation anomalies and the observed OLR anomalies is striking. Using the empirical approximation that a 5.7 W m^{-2} negative OLR anomaly roughly corresponds to a positive 1 mm day^{-1} precipitation anomaly (Arkin, personal communication, 1984), it is found that the magnitude of the simulated rainfall anomalies is also close to that observed. We make this comparison with caution because the above approximation was derived over a limited area (5°N–5°S, 160°E–160°W) using 8 years of OLR and station precipitation data.

The simulated precipitation anomalies were quite similar among the experiments as can be seen in Figs. 3b–d. There is an obvious direct relation between the positive precipitation differences and the extent of the very warm (~29°C) SST in the anomaly simulation (Fig. 1c). This is qualitatively in agreement with the results of Shukla and Wallace (1983), however the anomalous regions are of much greater extent in the current study. These precipitation differences developed quickly (within 2 weeks) and persisted throughout the course of the experiment. The precipitation differences are reflected in the 11–60 day ensemble average total atmospheric diabatic heating fields for the control (Fig. 4a) and anomaly (Fig. 4b) simulations. The diabatic heating differences were greatest in the mid-troposphere (not shown). The strength of the widespread anomalous heating is reflected in the zonally averaged 30°S–30°N, 200–1000 mb ensemble average thickness time series (Fig. 5a), which shows a positive difference steadily growing to a magnitude of 65 geopotential meters by the end of the experiments. The removal of the climate drift towards higher tropical temperature present in the earlier version of the model is evident when comparing this time series to Fig. 5b (taken from Shukla and Wallace, 1983).

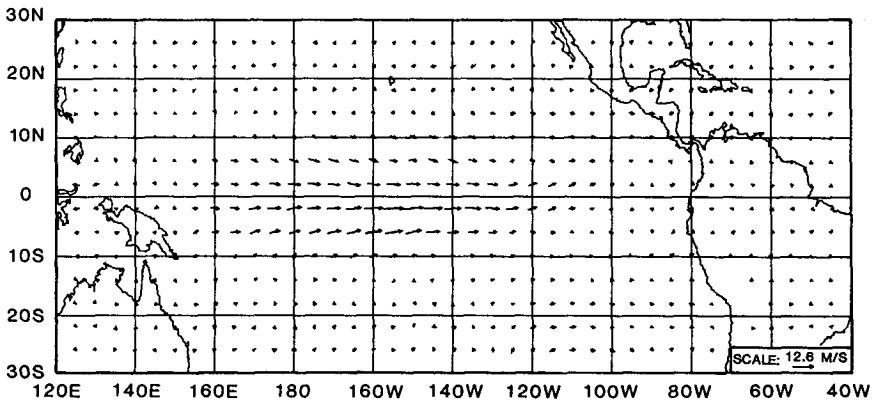

FIG. 7. 11–60 day ensemble average anomaly-minus-control 850 mb vector wind difference. Maximum = 12.6 m s^{-1}.

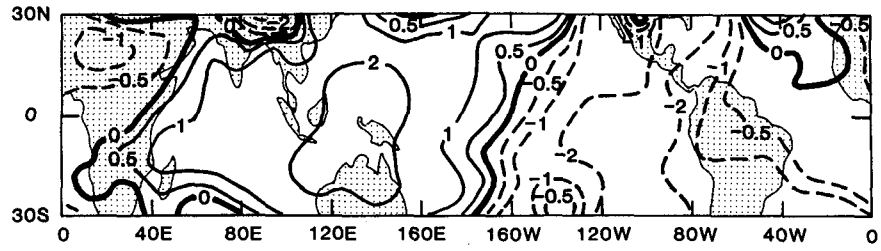

FIG. 8. 11–60 day ensemble average anomaly-minus-control sea level pressure difference. Contours are ±0.5, 1, 2, 4 mb. Dashed contours are negative.

b. Evaporation and moisture convergence

The 11–60 day ensemble average evaporation differences (Fig. 6a) reached around 4 mm day^{-1} over the regions of warmest SST in the anomaly simulation. Thus, the main contributor to the greatly enhanced precipitation was the highly anomalous vertically integrated moisture convergence (Fig. 6b) which had its greatest differences in the 800–1000 mb layer. This agrees with the results of Shukla and Wallace (1983), and it is mainly due to the enhanced low level equatorial westerlies to the west of the SST anomaly (Fig. 7). The large evaporation differences were due to the combined effects of warmer SST and stronger surface winds.

c. Sea level pressure

The sea level pressure (SLP) differences showed a strong (~2 mb) Southern Oscillation signal, as seen in the 11–60 day ensemble average difference (Fig. 8). This suggests that the SST anomalies are capable of producing the sea level pressure pattern of the Southern Oscillation as observed in the mature stage of an El Niño event.

d. Geopotential height and wind fields at upper levels

From such a strong and widespread tropical heating anomaly one might, in the light of linear theory and past observations, naturally expect to see extratropical responses. All three experiments had anomalous anticyclonic circulations aloft straddling the equator in the eastern Pacific, although they were much weaker and shifted eastward compared to those observed. The ~10 degree eastward shift of the anticyclonic couplet observed from January to February was approximately simulated in each experiment. A PNA-like pattern is evident in the observed 200 mb Northern Hemisphere height anomaly field for January 1983, although by February, the anomalous pattern, though still very strong, undergoes large changes.

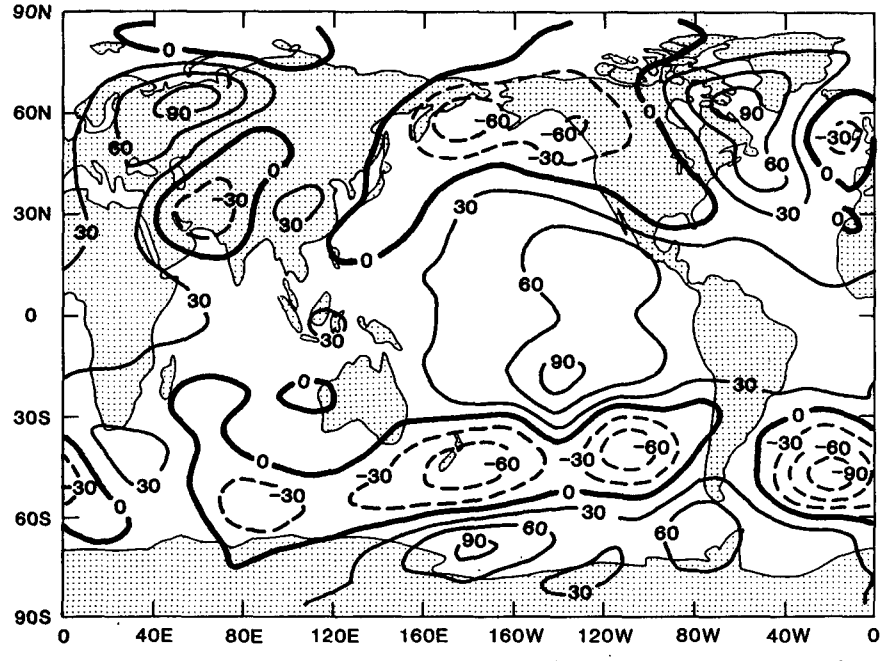

FIG. 9. 11–60 day ensemble average 1982–83 anomaly-minus-control 300 mb geopotential height difference. Units are geopotential meters. Dashed contours are negative.

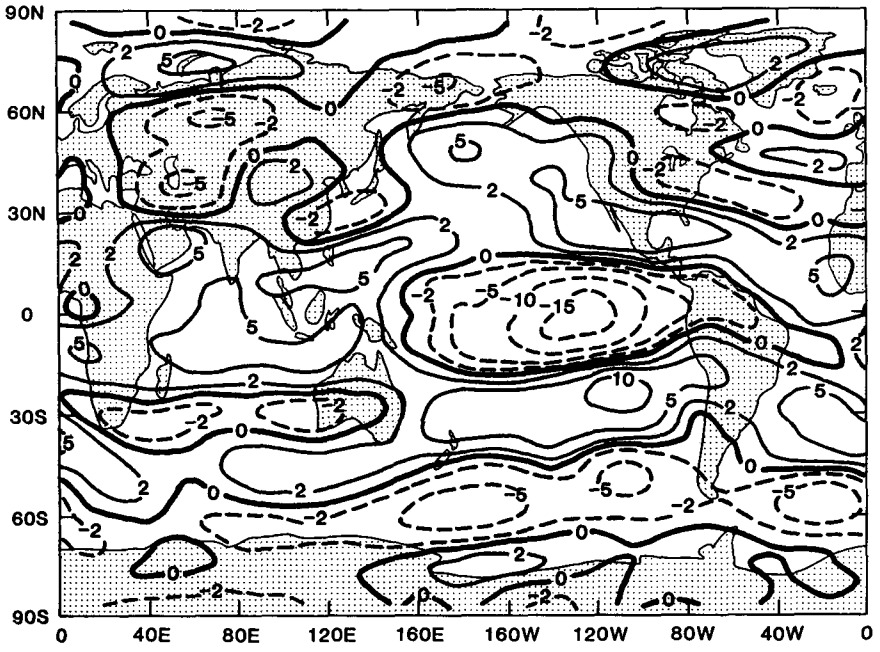

FIG. 10. 11–60 day ensemble anomaly-minus-control 300 mb zonal wind difference. Contours are ±2, 5, 10, 15, 20 m s^{-1}. Dashed contours are negative.

The 11–60 day ensemble average 300 mb geopotential height difference field (Fig. 9) shows a pattern over North America which resembles more the observed February or March anomaly pattern rather than the PNA or January pattern. This could perhaps be explained by the eastward extension of the anomalous precipitation in the simulations, which did not occur in the observations until several months later. Although these extratropical anomalies were consistently equivalent barotropic, there was a large variance in their locations among the experiments. None of the patterns over North America were significant at 95% on a univariate *t*-test (Chervin and Schneider, 1976). However, the increased heights throughout the tropical belt, the pattern off the southern tip of South America, and the large positive region over NW Eurasia were all significant at 99% on this same test.

The observed 200 mb zonal wind field for winter 1983 (not shown) had a large (~20 m s^{-1}) negative anomaly over the central and eastern equatorial Pacific, flanked by large (~20 m s^{-1}) positive anomalies at roughly 30°S and 30°N. The 11–60 day ensemble average 300 mb zonal wind difference field (Fig. 10) shows that the negative anomaly was correctly simulated, although the positive anomalies flanking it are both too weak and shifted eastward as compared to the observed anomalies. However, it does seem that the model, at least qualitatively, correctly simulated the local strengthening of the subtropical jet of either hemisphere.

At this point it should be mentioned that aside from the variance in extratropical anomalies, there was good agreement among the three sets of anomaly-minus-control difference fields for the three separate experiments. This similarity is particularly interesting considering the 60 day simulation started on 1 January 1975, which is the same initial condition used in one of the Shukla and Wallace (1983) integrations. This suggests a dominant effect of the surface boundary conditions as opposed to the initial conditions on the model simulations.

In conclusion, the results in the tropics seem clear. The SST anomalies force anomalous precipitation and heating over the areas of very warm (≥29°C) SST. In addition, they result in anomalous low-level westerlies and upper-level easterlies in the equatorial Pacific. The upper-level easterlies are related to a forced anomalous upper-level anticyclone couplet straddling the equator. The SST anomalies produce the SO signal of sea level pressure correctly.

The extratropical results are not nearly so clear. There is a strong extratropical response, although it varies greatly with both time and initial conditions. The first couple of weeks of the 1982–83 experiment did show a PNA-like pattern in the 300 mb geopotential height difference field. These results suggest the need for further studies with simpler models and observations to understand the mechanisms which determine the influence of tropical heating anomalies on midlatitude circulation.

Acknowledgments. The authors would like to thank Dr. Richard Reynolds of the Climate Analysis Center for providing the sea surface temperature data used

in this study. We would also like to thank Ms. Lora Thompson for her careful typing of the manuscript, and Ms. Laura Rumburg for drafting the figures.

REFERENCES

Arakawa, A., 1969: Parameterization of cumulus convection. *Proc. WMO/IUGG Symp. on Numerical Prediction,* Tokyo, 1-6.

Blackmon, M. L., J. E. Geisler and E. J. Pitcher, 1983: A general circulation model study of January climate anomaly patterns associated with interannual variation of equatorial Pacific sea surface temperatures. *J. Atmos. Sci.,* **40,** 1410–1425.

Chervin, R. M., and S. H. Schneider, 1976: On determining the statistical significance of climate experiments with general circulation models. *J. Atmos. Sci.,* **33,** 405–412.

Deardorff, J. W., 1972: Parameterization of the planetary boundary layer for use in general circulation models. *Mon. Wea. Rev.,* **100,** 93–106.

Julian, P. R., and R. W. Chervin, 1978: A study of the Southern Oscillation and Walker circulation phenomenon. *Mon. Wea. Rev.,* **106,** 1433–1451.

Keshavamurty, R. N., 1982: Response of the atmosphere to sea surface temperature anomalies over the equatorial Pacific and the teleconnections of the Southern Oscillation. *J. Atmos. Sci.,* **39,** 1241–1259.

Mintz, Y., and V. Serafini, 1981: Monthly normal global fields of soil moisture and land-surface evapotranspiration. *Int. Symp. on Variations in the Global Water Budget,* Oxford, International Union for Quarternary Research, Palev-Climate Commission, Reidel.

National Meteorological Center Climate Analysis Center, 1982–83: Special Climate Diagnostics Bulletins, No. 1–6.

Quiroz, R. S., 1983: The climate of the "El-Niño" winter of 1982–83, a season of extraordinary climatic anomalies. *Mon. Wea. Rev.,* **111,** 1685–1706.

Randall, D. A., 1976: *The interaction of the planetary layer with large-scale circulations.* Ph.D. thesis, UCLA, 247 pp.

——, 1982: Monthly and seasonal simulations with the GLAS climate model. *Proc. Workshop on Intercomparison of Large-Scale Models Used for Extended Range Forecasts of the European Centre for Medium-Range Weather Forecasts,* Reading, ECMWRF, 464 pp.

Rowntree, P. R., 1972: The influence of tropical east Pacific Ocean temperatures on the atmosphere. *Quart. J. Roy. Meteor. Soc.,* **98,** 290–321.

Shukla, J., and J. M. Wallace, 1983: Numerical simulation of the atmospheric response to equatorial Pacific sea surface temperature anomalies. *J. Atmos. Sci.,* **40,** 1613–1630.

——, D. Straus, D. Randall, Y. Sud and L. Marx, 1981: Winter and summer simulations with the GLAS climate model. NASA Tech. Memo. 83866, 282 pp. [NTIS N8218807.]

Wallace, J. M., and D. S. Gutzler, 1981: Teleconnections in the geopotential height field during the Northern Hemisphere winter. *Mon. Wea. Rev.,* **109,** 784–812.